Top Catal (2009) 52:140–147
DOI 10.1007/s11244-008-9150-8

ORIGINAL PAPER

Comparison of Activity and Selectivity of SSZ-33 Based Catalyst with other Zeolites in Toluene Disproportionation

S. Al-Khattaf · Z. Musilová-Pavlačková · M. A. Ali · J. Čejka

Published online: 23 December 2008

Abstract SSZ-33 based-catalyst, after modification with Mo and alumina binder, was evaluated in long-run tests in the toluene disproportionation in the presence of hydrogen as a carrier gas. The activity and selectivity of this catalyst were compared with those of ZSM-5 and mesoporous ZSM-5 prepared with the same concentration of Mo and alumina. Formation of the final catalysts decreased the void volume of micropores in order SSZ-33 > ZSM-5 > ZSM-5/Meso. Simultaneously, the concentration of Lewis acid sites increased due to the addition of alumina to the catalyst. The highest toluene conversion was achieved with SSZ-33 catalyst comprising 12-12-10-ring channels, which is the result of high acidity of this zeolite together with increased mass transport through large pores. ZSM-5 zeolite exhibited lower toluene conversion while only a low activity was found for mesoporous ZSM-5 probably due to the limitations of the access to the zeolite channels after modification with alumina.

Keywords SSZ-33 · ZSM-5 · Mesoporous ZSM-5 · Molybdenum · Toluene disproportionation · Reaction temperature

S. Al-Khattaf · M. A. Ali
Center of Research Excellence in Petroleum Refining and Petrochemicals at King Fahd University of Petroleum and Minerals (KFUPM), Dhahran, Saudi Arabia

Z. Musilová-Pavlačková · J. Čejka (✉)
J. Heyrovský Institute of Physical Chemistry ASCR, v.v.i., Dolejškova 3, 182 23 Prague, Czech Republic
e-mail: jiri.cejka@jh-inst.cas.cz

1 Introduction

Micro and mesoporous materials are playing an important role in adsorption, separation and particularly in catalysis both in laboratory as well as industrial scale. These porous materials include mainly zeolites, mesoporous molecular sieves and recently also metal organic frameworks (MOFs), which provide a high number of possibilities to design new type of catalysts [1–4].

Transformations of aromatic hydrocarbons over zeolites play very important role in upgrading of less valued aromatic hydrocarbons to highly required ones. Disproportionation of toluene belongs to such type of important value-added reactions, in which low-value toluene is transformed into a mixture of xylenes [5, 6]. Xylenes are industrially used as a raw material for a number of petrochemical processes [7]. During the toluene disproportionation reaction (TDP), mixture of benzene and individual xylene isomers is produced, the concentration of which strongly depends on the type of catalyst employed [8]. The *ortho*-xylene and *meta*-xylene are processed further by isomerization reaction to produce *para*-xylene, which is used for the production of polyester fibers, resins, and films [9]. Because of the increasing demand for *para*-xylene, new technologies and routes are searched to convert low value hydrocarbons to more demanded ones and toluene disproportionation to *para*-xylene is one of the typical examples.

A number of different zeolites such as Y, ZSM-5, mordenite, and MCM-22 have been reported in the literature for toluene or ethylbenzene disproportionation reactions [10–14]. Catalytic activity has been enhanced using lower silicon-to-aluminum ratio zeolites [10]. Different zeolites ion-exchanged with nickel, lead, and chromium have been reported for TDP. The *p*-xylene yield increased after the ion-exchange and the maximum was

obtained with chromium-loaded HZSM-5 at 600 °C under atmospheric pressure [15]. The *p*-xylene selectivity in TDP reaction has been also enhanced by replacing the zeolite proton by InO^+ cations [16]. Tsai [17] reported a novel method using hydrogen to reactivate the active sites on coked mordenite. It has been reported that in fluidized bed using Y zeolite, toluene conversion takes place through disproportionation reaction in trace level when the acidity of the zeolite is low. In the case of Y zeolite having high acidity, toluene transformation favors the dealkylation and paring reactions producing more gases [18]. It is well documented that in zeolite based catalysts *p*-xylene selectivity can be increased via blocking the active sites at the external surface outside the pores and the reaction is forced to occur inside the pores [19]. Olson and Haag [20] stressed also the role of the diffusional path length by studying the effect of zeolite crystal size on the activity in TDP.

The effect of the reaction pressure on the toluene disproportionation reaction using ZSM-5 zeolite based catalyst impregnated with molybdenum was investigated by Al-Khattaf et al. [21]. Toluene conversion was found to increase with increasing reaction pressure and reaction temperature while deactivation of the catalyst was faster in nitrogen compared with hydrogen as carrier gas being indicated by a higher amount of coke formation [21]. Toluene is also an important component for transalkylation with trimethylbenzenes to provide xylenes. 1,2,4-Trimethylbenzene (TMB) transalkylation with toluene has been studied over USY zeolite type catalyst [22]. Reaction mixture of 50:50 wt% TMB and toluene was used. The apparent activation energies for bimolecular transalkylation reactions were found to decrease as follows: *E*(transalkylation) > *E*(isomerization) > *E*(disproportionation). Substantially higher reactivity of trimethylbenzenes compared with toluene was confirmed over different structural types of zeolites, namely beta, mordenite, and Y [23].

Zeolite SSZ-33 (CON topology) possesses a channel system compiled of intersecting 12-MR (member ring) and 10-MR pores; it is the first synthetic zeolite having 4–4 = 1 SBU (secondary building unit) in the structure [24]. Acidity of this novel zeolite was recently discussed based on FTIR study with different probe molecules as for their size and basicity and ^{1}H and ^{27}Al MAS NMR [25]. SSZ-33 also exhibits a high catalytic activity in ferrocene acylation with acetic anhydride [26]. Mesoporous ZSM-5 also tested in this reaction represents a novel type of zeolitic material with pre-formed mesopores by adding carbon nanoparticles to the synthesis gel [27–29].

The objective of this paper is to compare the catalytic activity of a novel zeolite SSZ-33 possessing 12-12-10-MR system with pure microporous ZSM-5 and mesoporous ZSM-5 in toluene disproportionation. ZSM-5 zeolite was chosen because of the fact that it has been proved very active and selective for toluene disproportionation reaction and has shown less coke deposition as compared to other types of zeolites. Each zeolite was modified by the same way with Mo and alumina as a binder to get the final catalysts. Disproportionation reaction was carried out under hydrogen to observe the effect of the time-on-stream (T-O-S) on the toluene conversion and xylenes selectivity. The commercial process utilizes 30 bar of hydrogen pressure in the presence of zeolite based catalysts. To find the interplay between the activity of final catalysts and their acidity, all parent zeolites and final catalysts were evaluated as for their textural properties by sorption of nitrogen and the number and type of acid sites by FTIR spectroscopy.

2 Experimental

2.1 Zeolite Synthesis

The SSZ-33 zeolite was synthesized according to the patent [30] using the template molecule derived from 8-keto tricycle [5.2.1.0] decane. The *endo* isomer is the active structure directing agent for making this zeolite [31].

Into a 19-L reactor 3500 mL of water was first added and then 1.8 mol of the SDA in 3700 mL of water. Boric acid (89 g) was dissolved and subsequently 38 g of solid NaOH was added. Finally, after a clear solution was obtained, ca. 9 moles of Cab–O–Sil M5 (97% SiO_2, Cabot) was added. The reaction mixture was stirred at 75 rpm and brought to 160 °C over a programmed 12 h ramp up. The reaction was maintained for 10 days and then the reactor was cooled down. The synthesized SSZ-33 was calcined in an oven with a stream of nitrogen gas passing over the zeolite in thin coverage on trays. The program was run at 1 °C/min to 120 °C, maintained at 120 °C for 2 h then heated (1 °C/min) to 540 °C, kept for 5 h, and further heated to 595 °C (1 °C/min) and maintained for another 5 h.

Transformation of (B)SSZ-33 to (Al)SSZ-33 was carried out by a one-step reflux in 1 M aluminum nitrate. Details about the procedure were reported in the work by Chen et al. [32]. The Si/Al ratio of SSZ-33 sample under study was equal to 18.

Synthesis of ZSM-5 zeolite and its mesoporous counterpart were carried out in the following way. ZSM-5 was synthesized hydrothermally using gel composition of 1 Al_2O_3:70 SiO_2:25.5 TPAOH:70 EtOH:2596 H_2O. Tetraethyl orthosilicate (TEOS, Fluka) and aluminum nitrate nonahydrate ($Al(NO_3)_3 \cdot 9H_2O$, Fluka) were used as the source of silicon and aluminum, respectively. Tetrapropylammonium hydroxide (TPAOH, 20% in water, Aldrich) was used as template. For the synthesis of mesoporous ZSM-5 (MesoZSM-5) Carbon Black Pearls (CBP 2000, carbon particle diameter of 12 nm, Cabot Corp.) were used

as secondary template to form the mesoporous structure. In a typical procedure, $Al(NO_3)_3 \cdot 9H_2O$ was dissolved in a small amount of H_2O followed by the addition of TEOS and ethanol (EtOH, 96%, Fluka). After vigorous stirring for 1.5 h, TPAOH dissolved in water was added and the mixture was stirred for another 1.5 h. Then the resulting gel was transferred into 90 mL autoclaves. When mesoporous ZSM-5 was aimed to prepare, CBP 2000 dried at 120 °C overnight was added to the mixture and homogenized for additional 3 h. In both cases, the crystallization was carried out under static conditions in Teflon-lined autoclaves at 170 °C for 6 days. After crystallization, the solid phase was recovered by filtration, washed out with deionized water and dried at 90 °C overnight. The template and carbon black were removed by calcination at 550 °C for 24 h with a temperature ramp of 1 °C/min. Ammonium forms of these zeolites were prepared via four-time repeated ion-exchange of these samples in 0.5 M aqueous solution of ammonium nitrate. Si/Al molar ratio of ZSM-5 zeolite and mesoporous ZSM-5 are 60 and 64 (by FT-IR), respectively.

2.2 Catalyst Preparation

For the preparation of the catalysts under study, alumina binder (Cataloid AP-3) was used to prepare the catalyst extrudates. Cataloid AP-3 contains 75.4 wt% alumina, 3.4 wt% acetic acid and water as a balance. The preparation procedure was as follows: alumina binder was dispersed in water and stirred for 30 min to produce thick slurry. The zeolite powder was then mixed with the alumina slurry to produce a thick paste. The paste was subjected to an extruder to produce 1 mm thickness extrudates. These were dried at room temperature for 4 h and then dried at 120 °C for 2 h, followed by calcinations at 500 °C for 2 h in a temperature programmed furnace.

Finally, aqueous solution containing hexaammonium heptamolybdate tetrahydrate was used to impregnate all the catalysts extrudates with 3% of molybdenum. The metal loaded extrudates were dried at room temperature and at 120 °C, and finally calcined at 500 °C. The composition of the catalysts under study is as follows:

Table 1 provides list of catalysts studied and their codes

2.3 Zeolite and Catalyst Characterization

The crystallinity of zeolites was determined by X-ray powder diffraction with a Bruker D8 Advance X-ray powder diffractometer equipped with a graphite monochromator and position sensitive detector using CuKα radiation in Bragg-Brentano geometry. The shape and size of zeolite crystals were determined by scanning electron microscopy (Jeol, JSM-5500LV).

Table 1 Composition of zeolite based catalysts under study

Catalyst designation	Composition
C-SSZ-33	3%Mo/[SSZ-33 (66%) and AP-3 (33%)]
C-ZSM-5	3%Mo/[ZSM-5 (66%) and AP-3 (33%)]
C-MesoZSM-5	3%Mo/[MesoZSM-5 (66%) and AP-3 (33%)]

Acidity of all zeolites was investigated by adsorption of d_3-acetonitrile used as probe molecule followed by FTIR spectroscopy. All zeolites and catalysts were activated in a form of self-supporting wafers (8–12 mg/cm^2) at 450 °C overnight. The adsorption of d_3-acetonitrile was carried out at ambient temperature. Adsorption of d_3-acetonitrile was investigated on a Nicolet Protégé 460 spectrometer with a resolution of 4 cm^{-1}.

Adsorption isotherms of nitrogen at −196 °C were measured with a Micromeritics ASAP 2020 instrument. Prior to the adsorption measurements, all samples were degassed at 250 °C until pressure of 0.001 Pa was attained.

2.4 Catalyst Evaluation

All catalysts were evaluated in toluene disproportionation carried out in a fixed-bed reaction system at liquid hour space velocity (LHSV) of 1.5 h^{-1}. Reaction was studied under 30 bars of hydrogen pressure at the reaction temperature of 400 °C. Each run continued for 88 h of T-O-S to see the effect of T-O-S on toluene conversion, product selectivity and catalyst deactivation. The procedure of the catalyst testing and product analyses was as follows: 15 mL of each catalyst was charged in the middle part of the reactor (total volume 50 mL) provided with inert in the upper and lower portion of the reactor. Prior to loading, the catalyst was calcined at 500 °C for 3 h. The reactor was heated at the rate of 5 °C/min and the catalyst was activated at high temperature in situ in the presence of hydrogen prior to the reaction. The toluene feed was then started and the temperature was brought to the desired reaction temperature. The reaction products were separated in a gas-liquid separator. Both gas and liquid samples were collected after a certain prescribed time, at which the reaction conditions were stabilized and the products collected were representative.

The liquid reaction products were analyzed using PI-ONA Analyzer based on a Shimadzu gas chromatograph GC-2010 with Shimadzu auto-sampler AOC-20i. The PI-ONA Analyzer was equipped with FID detector. The hydrocarbon separation was carried out on 50 m long and 0.15 mm diameter BP1PONA-M50-050 column under temperature programmed conditions. The components were identified using a calibration that was accomplished using a standard hydrocarbon mixture sample having the components of known composition. The gaseous

hydrocarbons, nitrogen and hydrogen were separated on alumina PLOT, 50 m capillary column. In gaseous samples collected and analyzed, no appreciable amounts of hydrocarbons were detected ad thus the results were not considered.

3 Results and Discussion

3.1 Catalyst Characterization

X-ray powder patterns of all zeolites under study exhibited good crystallinity and characteristic diffraction lines (not shown here). Also individual catalysts prepared from these zeolites exhibited only diffraction lines being typical for these structural types of zeolites (SSZ-33, ZSM-5).

Figure 1 shows typical SEM images of calcined zeolites SSZ-33, ZSM-5 and mesoporous ZSM-5. The images evidence the absence of any additional phase even an amorphous one. The size of the crystals of mesoporous ZSM-5 is around 1.5 μm while ZSM-5 provides crystals close to 0.3 μm. The crystals of SSZ-33 are close to this value being equal to 0.5 μm.

Textural properties of zeolites and final catalysts were evaluated based on nitrogen adsorption isotherms; for estimation of micropore volume t-plot method was applied (Table 2). Micropore volume for all zeolites decreased by 25–30% due to addition of a binder. While no structural collapse of zeolites is expected, this decrease corresponds to the amount of alumina binder used for modification. In contrast, mesopore volume increased for all catalysts after modification. While the "mesopore" volume for parent SSZ-33 and ZSM-5, 0.174 and 0.118 cm^3/g, respectively, can be assigned to interparticle volume, the value 0.265 cm^3/g for mesoporous ZSM-5 represents the highest value of real mesopores we ever prepared. Mesopore volume after preparation of catalysts increased for all materials. The values for C-SSZ-33 and C-ZSM-5 are almost doubled in comparison with parent zeolite, which indicates that modification with alumina led to the formation of some mesopores. However, mesopore volume of C-MesoZSM-5 only slightly increased compared with parent MesoZSM-5, 0.297 and 0.265, respectively. SEM image of MesoZSM-5 (Fig. 1) clearly depicts substantial surface roughness formed after the burning of carbon black particles used to create mesopores. Thus, we believe that the preparation of real catalyst led to the blocking of these surface "holes". As a result the increase in the void volume is only around 10%.

Infrared spectra of parent zeolites SSZ-33, ZSM-5 and MesoZSM-5 and final catalysts C-SSZ-33, C-ZSM-5 and C-MesoZSM-5 before and after adsorption of d_3-acetonitrile are depicted in Fig. 2. For all parent zeolites typical

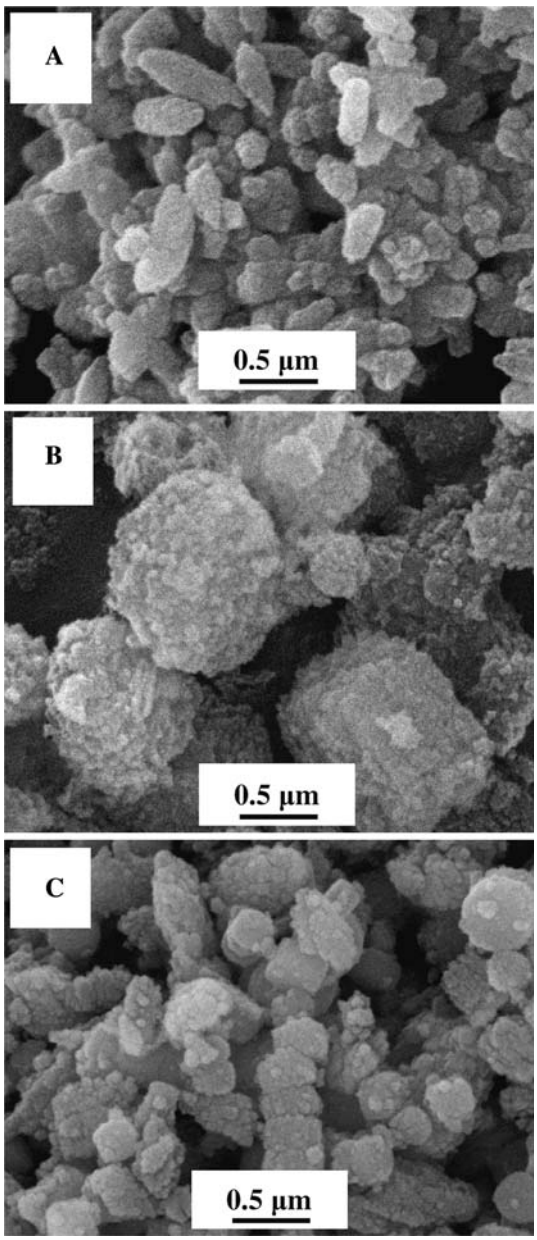

Fig. 1 SEM images of SSZ-33 (**a**), MesoZSM-5 (**b**) and ZSM-5 (**c**)

Table 2 Textural parameters of zeolites and catalysts evaluated

Sample code	V_{MI}[a] (cm^3/g)	V_{ME}[b] (cm^3/g)	S_{ME}[c] (m^2/g)
ZSM-5	0.121	0.118	152
C-ZSM-5	0.093	0.235	163
MesoZSM-5	0.097	0.265	169
C-MesoZSM-5	0.067	0.296	182
SSZ-33	0.206	0.174	114
C-SSZ-33	0.148	0.294	124

[a] V_{MI}—micropore volume

[b] V_{ME}—mesopore volume

[c] S_{ME}—mesopore surface area

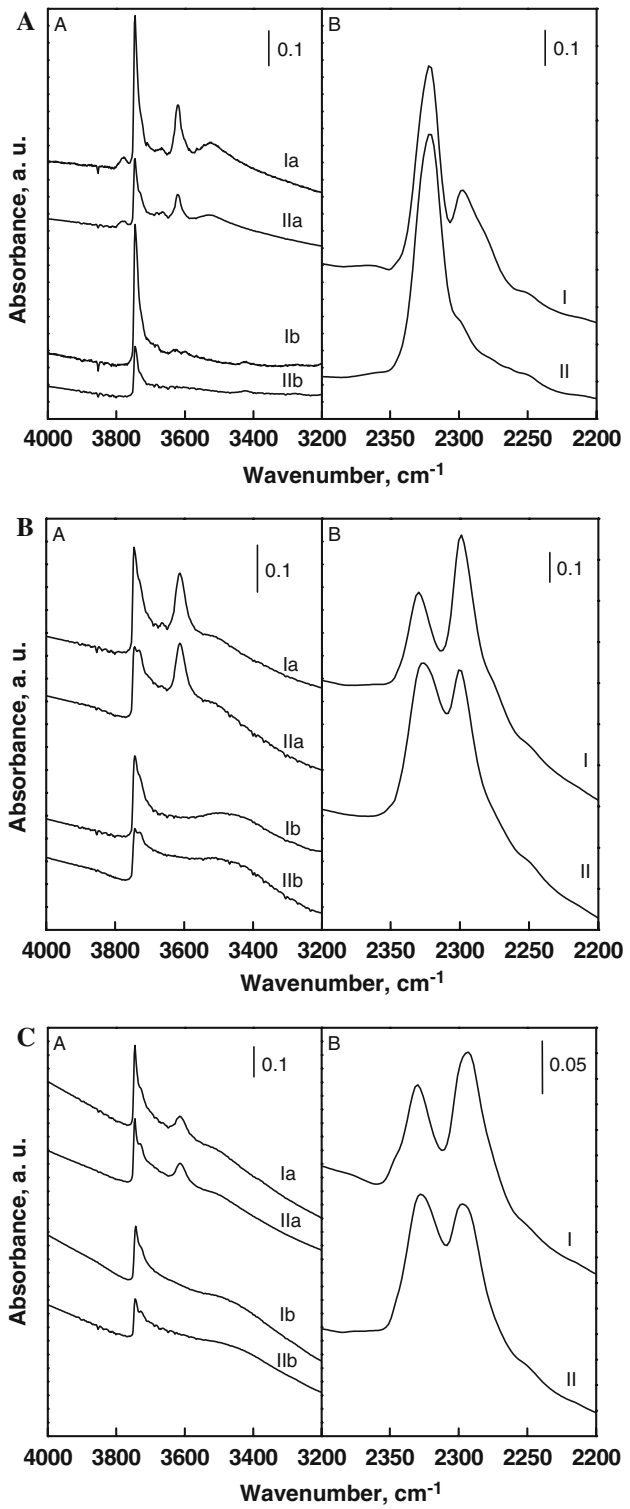

◀ **Fig. 2** **A** IR spectra of hydroxyl vibration region of SSZ-33 (I) and C-SSZ-33 (II) zeolite, before (a) and after (b) d_3-acetonitrile adsorption (**A**) and spectra of d_3-acetonitrile region after its adsorption (**B**). **B** IR spectra of hydroxyl vibration region of ZSM-5 (I) and C-ZSM-5 (II) zeolite, before (a) and after (b) d_3-acetonitrile adsorption (**A**) and spectra of d_3-acetonitrile region after its adsorption (**B**). **C** IR spectra of hydroxyl vibration region of MesoZSM-5 (I) and C-MesoZSM-5 (II) zeolite, before (a) and after (b) d_3-acetonitrile adsorption (**A**) and spectra of d_3-acetonitrile region after its adsorption (**B**)

absorption bands of silanol groups at 3742–5 cm^{-1} and acidic bridging Si-OH-Al groups at 3610–3615 cm^{-1} were observed. Detailed discussion of infrared spectra of SSZ-33 is provided elsewhere [25]. After the adsorption of d_3-acetonitrile the absorption bands of bridging groups were eliminated but new bands characteristic of d_3-acetonitrile C≡N bond interacting with Brønsted and Lewis acid sites appeared. Table 3 shows the concentrations of the individual types of acid sites and the Si/Al ratio determined using FTIR. The preparation of the final catalysts led to a decrease in the intensity of Si–OH silanol groups due to an interaction with alumina binder. Simultaneously, lower concentrations of acidic bridging groups were found. It indicates that mixing of zeolites with alumina binder decreases the concentration of bridging OH groups and this decrease is larger than that, which can be expected for external surface of zeolite crystals. Particularly, in the case of SSZ-33 zeolite (Fig. 2a) this decrease is much larger than for ZSM-5 zeolite (Fig. 2b). Bridging OH groups are preferentially located inside of 12-MR (see Ref. [25]), which indicates that some of these groups are blocked by alumina binder. Table 3 providing quantitative evaluation of FTIR spectra of parent zeolites and final catalysts, allows us to draw several important conclusions:

(i) the concentration of framework aluminum (Si/Al) in zeolites is always higher than in the reaction gel,
(ii) although ZSM-5 and MesoZSM-5 were synthesized from the same reaction gel, the amount of aluminum incorporated into MesoZSM-5 is lower compared with ZSM-5,
(iii) addition of alumina binder led to the decrease in Si/Al ratio for all catalysts and to a simultaneous increase in the concentration of Lewis acid sites,
(iv) the concentration of Brønsted acid sites in C-MesoZSM-5 compared with MesoZSM-5 decreased only slightly, which indicates that Brønsted acid sites are probably not located close to the mesopores formed around carbon black particles.

3.2 Toluene Disproportionation

Figure 3 provides T-O-S dependence of toluene conversion over zeolite based catalysts prepared from SSZ-33, ZSM-5 and mesoporous ZSM-5 materials. The initial conversions of toluene in TDP carried out at 400 °C follow the order C-SSZ-33 (62%) > C-ZSM-5 (41%) > C-MesoZSM-5 (18%). Toluene conversion was practically constant during the whole run as a result of Mo addition and using hydrogen as carrier gas. This fact provides us with a nice

Table 3 Si/Al ratios in the initial reaction mixture and in the parent zeolite and final catalyst, concentration of Brønsted and Lewis acid sites of zeolites and catalysts under study

Sample code	Si/Al gel	Si/Al (FT-IR)	Lewis sites mmol/g	Brønsted sites mmol/g	Lewis sites (%)	Brønsted sites (%)
ZSM-5	35	60	0.07	0.13	34	66
C-ZSM-5	–	43	0.14	0.11	70	30
MesoZSM-5	35	64	0.06	0.13	32	68
C-MesoZSM-5	–	55	0.09	0.11	44	56
SSZ-33	15	18	0.40	0.18	70	30
C-SSZ-33	–	16	0.44	0.09	83	17

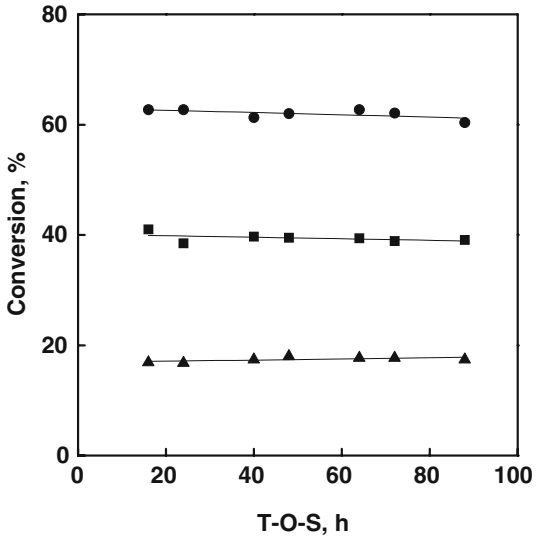

Fig. 3 Time-on-stream dependence of toluene conversion in toluene disproportionation over C-SSZ-33 (●), C-ZSM-5 (■) and C-MesoZSM-5(▲)

opportunity to compare the catalytic data obtained on our catalysts with textural and acidic properties practically without any influence of deactivation. When relating toluene conversion to the micropore volume of all catalysts (Table 2) we can see that C-SSZ-33 exhibits the highest micropore volume followed by C-ZSM-5 and C-MesoZSM-5. The same order of micropore volumes was found for the parent zeolites. Similarly, toluene conversion depends on the concentration and acid strength of Brønsted and Lewis acid sites in the catalysts. Both SSZ-33 and ZSM-5 zeolites exhibit quite high acid strength of their acid sites, thus, different concentrations but not the strength of the individual sites should be related to the different toluene conversions. Again, the Si/Al ratios in the final catalysts are in the same order, C-SSZ-33 > C-ZSM-5 > C-MesoZSM-5 (Table 3). Based on the comparison of the role of micropore volume and acidity on toluene conversion in toluene disproportionation it can be inferred that more open structure of SSZ-33 based catalyst (12-12-10-MR) allows a higher reaction rate and faster diffusion of both reactants and products in comparison with the medium pore (10-MR) ZSM-5 zeolite. Higher toluene conversion over C-ZSM-5 than C-MesoZSM-5 is probably due to a blocking of the surface roughness, formed after removal of carbon particles operating as secondary template during the synthesis, on the external surface of MesoZSM-5 crystals by alumina binder.

Toluene disproportionation leads to benzene and mixture of xylenes and should result in benzene/xylene molar ratio equal to one when no parallel or consecutive reactions take place. These undesired reactions include dealkylation leading to light hydrocarbons (gaseous products) and various methyl transfer reactions leading to higher aromatics like C_9 fraction. Benzene/xylene molar ratios were around 1.5 for C-ZSM-5, 1.4 for C-MesoZSM-5 and 1.6–1.7 for C-SSZ-33 (Fig. 4). The increase in the benzene/xylene ratio is parallel with increasing toluene conversion. This indicates that for more active catalysts dealkylation and transalkylation reactions are more important. In the case of C-SSZ-33, non-aromatics formed 10–12 mol% of products compared with 4–5% for C-ZSM-5 and only 3.5% for C-MesoZSM-5, which clearly reflects the level of toluene conversion (Fig. 5). The level of toluene conversion and size of the channels are clearly related to the concentration of C_9 fraction formed. While for C-MesoZSM-5 and C-ZSM-5 catalysts, the amounts of C_9 fraction are 0.5–0.9% and 1.2–1.5%, for C-SSZ-33, it is 5–6%. It is clear that 12-MR channels and their intersections allows not only the formation of bulky intermediates but also desorption of different trimethylbenzene isomers (TMB) or ethyltoluenes (ET). In the C_9 fraction 1,2,4-TMB dominates among trimethylbenzenes while 3-ET is preferred in ethyltoluene fraction. It means that while for TMBs some kinetic effect should be considered (shape selectivity) in the case of ethyltoluenes, the thermodynamically most favored ET exhibits the highest selectivity.

Selectivity to the sum of xylenes follows the order C-ZSM-5 (33–35%) > C-MesoZSM-5 (27–29%) > C-SSZ-33 (26–27%), cf. Fig. 4. It means that this order is not directly related to the toluene conversion but to the reaction

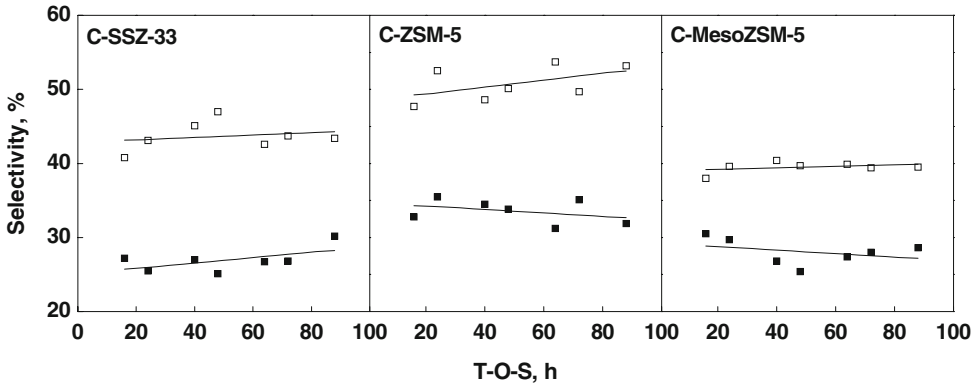

Fig. 4 Time-on-stream dependence of benzene (□) and total xylenes (■) selectivity in toluene disproportionation

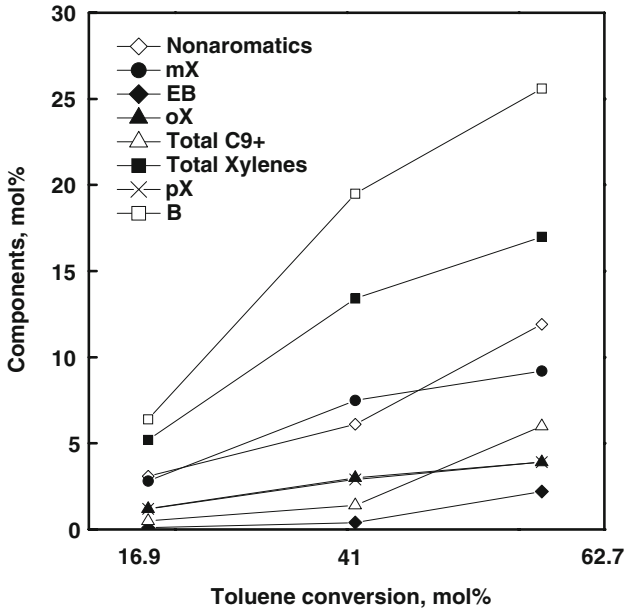

Fig. 5 Composition of the reaction products at 16 h time-on-stream as a function of different toluene conversions

volume. C-ZSM-5 with its three-dimensional system of 10-MR channels does not allow a substantial formation of bulky intermediates and mainly benzene and xylenes are formed. As for C-MesoZSM-5, the portion of mesopores inherent to the structure of MesoZSM-5 and their connectivity with micropores provides larger reaction volume enabling consecutive reactions of xylenes to proceed. SSZ-33 with interconnecting 12-MR allows relatively large reaction volumes for consecutive reactions as it was already discussed for C_9 fraction. The result of which is the lowest selectivity towards xylenes. No para-selectivity was found under our reaction conditions for any zeolite under study. The selectivity toward *p*-xylene in the xylenes mixtures was between 22% and 24%, which is close to the thermodynamic concentration of *p*-xylene in xylenes under reaction conditions applied.

4 Conclusions

Toluene disproportionation was investigated over zeolite based catalysts prepared from parent zeolites SSZ-33, ZSM-5 and mesoporous ZSM-5 by modification with molybdenum and alumina binder.

An increase in the concentration of Lewis acid sites was observed after modification of parent zeolites with alumina binder simultaneously with a decrease in the micropore volume. Alumina binder provided also some mesopores mainly for SSZ-33 and ZSM-5 while the increase in the mesopore volume over mesoporous ZSM-5 was rather low.

SSZ-33 based catalysts exhibited superior activity in toluene disproportionation. Toluene conversion over all three zeolite-based catalysts was constant for almost 100 h of time-on-stream and it follows the order of micropore volume and concentration of acid sites (C-SSZ-33 > C-ZSM-5 > C-mesoZSM-5).

The higher was the toluene conversion the higher was also the rate of competitive and consecutive reactions leading to non-aromatic products (via dealkylation/ring opening) or higher aromatic hydrocarbons (via transalkylations/disproportionation).

Acknowledgement The authors thank Dr. S. I. Zones (Chevron) for providing SSZ-33 zeolite and supporting this work. The Support provided by The Center of Research Excellence in Petroleum Refining and Petrochemicals at King Fahd University of Petroleum and Minerals (KFUPM) is appreciated. J. Čejka was supported by the Academy of Sciences of the Czech Republic (1QS400400560) while Z. Musilová-Pavlačková thanks the Grant Agency of the Czech Republic (203/08/H032) and Dr. L. Brabec for recording the SEM images.

References

1. Thomas M, Raja R (2007) Stud Surf Sci Catal 170:19
2. Degnan TF Jr (2007) Stud Surf Sci Catal 170:54
3. Férey G (2007) Stud Surf Sci Catal 170:66
4. Thomas JM (2008) J Chem Phys 128 Art Nr 182502
5. Čejka J, Wichterlová B (2002) Catal Rev 44:375

6. Bejblová M, Žilková N, Čejka J (2008) Res Chem Intermed 34:439
7. Tsai T-C, Liu S-B, Wang I (1999) Appl Catal A 181:355
8. Chen NY, Garwood WE, Dwyer FG (1996) Shape selective catalysis in industrial application. Marcel Dekker, New York
9. Franck H-G, Stadelhofer JW (1988) Industrial aromatic chemistry. Springer, Berlin
10. Uguina MA, Sotelo JL, Serrano DP (1991) Appl Catal 76:183
11. Tsai T-C, Chen WH, Liu S-B, Tsai C-H, Wang I (2002) Catal Today 73:39
12. Wichterlová B, Čejka J (1992) Catal Lett 16:421
13. Bhavani A, Karthekayen D, Rao A, Lingappan N (2005) Catal Lett 103:89
14. Mavrodinova VP, Papova MD, Neinska YG, Minchev CI (2001) Appl Catal A 210:397
15. Chaudhari PK, Saini PK, Chand S (2002) J Sci Ind Res 61:810
16. Mavrodinova VP, Papova MD (2005) Catal Commun 6:247
17. Tsai T-C (2006) Appl Catal A 301:292
18. Al-Khattaf S (2006) Energy Fuels 20:946
19. Chen NY, Kaeding WW, Dwyer FG (1979) J Am Chem Soc 101:6783
20. Olson DH, Haag WO (1984) Symp Ser 248:275
21. Al-Khattaf S, Ali MA, Al-Amer A (2008) Energy Fuel 22:243
22. Al-Khattaf S, Tukur NM, Al-Amer A (2007) Ind Eng Chem Res 46:4459
23. Čejka J, Kotrla J, Krejčí A (2004) Appl Catal A 277:191
24. Wagner P, Nakagawa Y, Lee GS, Davis ME, Elomari S, Medrud RC, Zones SI (2000) J Am Chem Soc 122:263
25. Gil B, Zones SI, Hwang SJ, Bejblová M, Čejka J (2008) J Phys Chem C 112:2997
26. Bejblová M, Zones SI, Čejka J (2007) Appl Catal A 327:255
27. Jacobsen CJH, Madsen C, Houžvička J, Schmidt I, Carlsson A (2000) J Am Chem Soc 122:7116
28. Hartmann M (2004) Angew Chem Int Ed 43:5880
29. Čejka J, Mintova S (2007) Catal Rev 49:457
30. Zones SI (1990) US Patent 4 963 337
31. Zones SI, Nakagawa Y, Yuen LT, Harris TV (1996) J Am Chem Soc 118:7558
32. Chen CY, Zones SI, Hwang SJ, Bull LM (2005) Stud Surf Sci Catal 154:1547